Modelling the persistent low-state γ-ray emission of the PKS 1510-089 blazar

Egor Podlesnyi,
Timur Dzhatdoev, Emil Khalikov,
Vasilisa Latypova, Igor Vaiman

Monthly Notices
of the
ROYAL ASTRONOMICAL SOCIETY

MNRAS **515**, 5242–5250 (2022) https://doi.org/10.1093/mnras/stac2094

Modelling the persistent low-state γ-ray emission of the PKS 1510−089 blazar with electromagnetic cascades initiated in hadronuclear interactions

T. A. Dzhatdoev,[1,2,3]★ E. V. Khalikov,[1] V. S. Latypova,[4] E. I. Podlesnyi[1,3,4] and I. A. Vaiman[1,3,4]

[1] *Federal State Budget Educational Institution of Higher Education, M.V. Lomonosov Moscow State University, Skobeltsyn Institute of Nuclear Physics (SINP MSU), 1(2), Leninskie gory, GSP-1, 119991 Moscow, Russia*

[2] *Institute for Cosmic Ray Research, University of Tokyo, 5-1-5 Kashiwanoha, Kashiwa, Japan*

[3] *Institute for Nuclear Research of the Russian Academy of Sciences, 7a, 60th October Anniversary Prospect, 117312 Moscow, Russia*

[4] *Federal State Budget Educational Institution of Higher Education, M.V. Lomonosov Moscow State University, Department of Physics, 1(2), Leninskie gory, GSP-1, 119991 Moscow, Russia*

Accepted 2022 July 22. Received 2022 July 22; in original form 2021 November 14

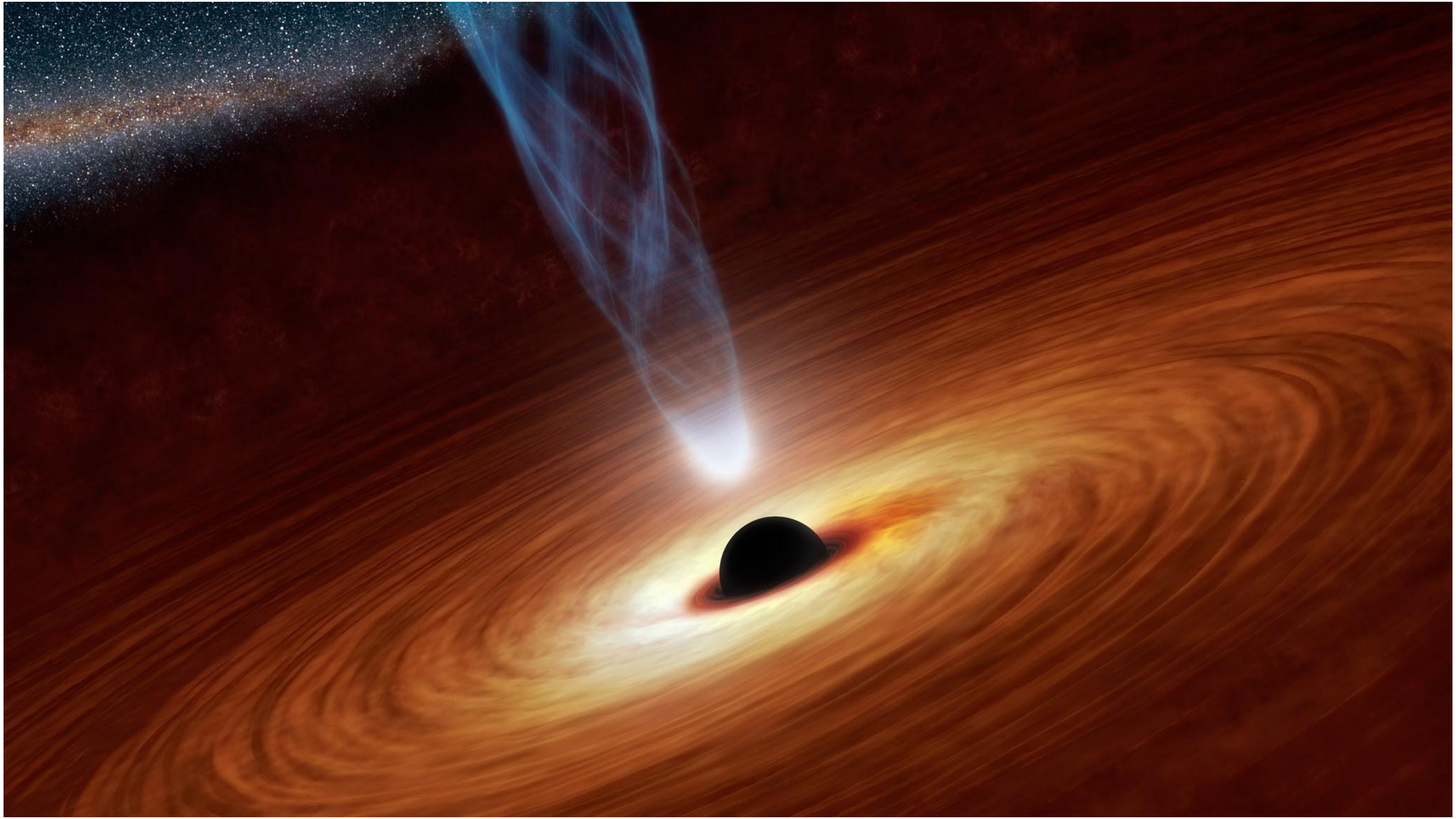

An artist’s impression of an active galactic nucleus (AGN)

Credit: NASA/JPL-Caltech

Blazar sequence

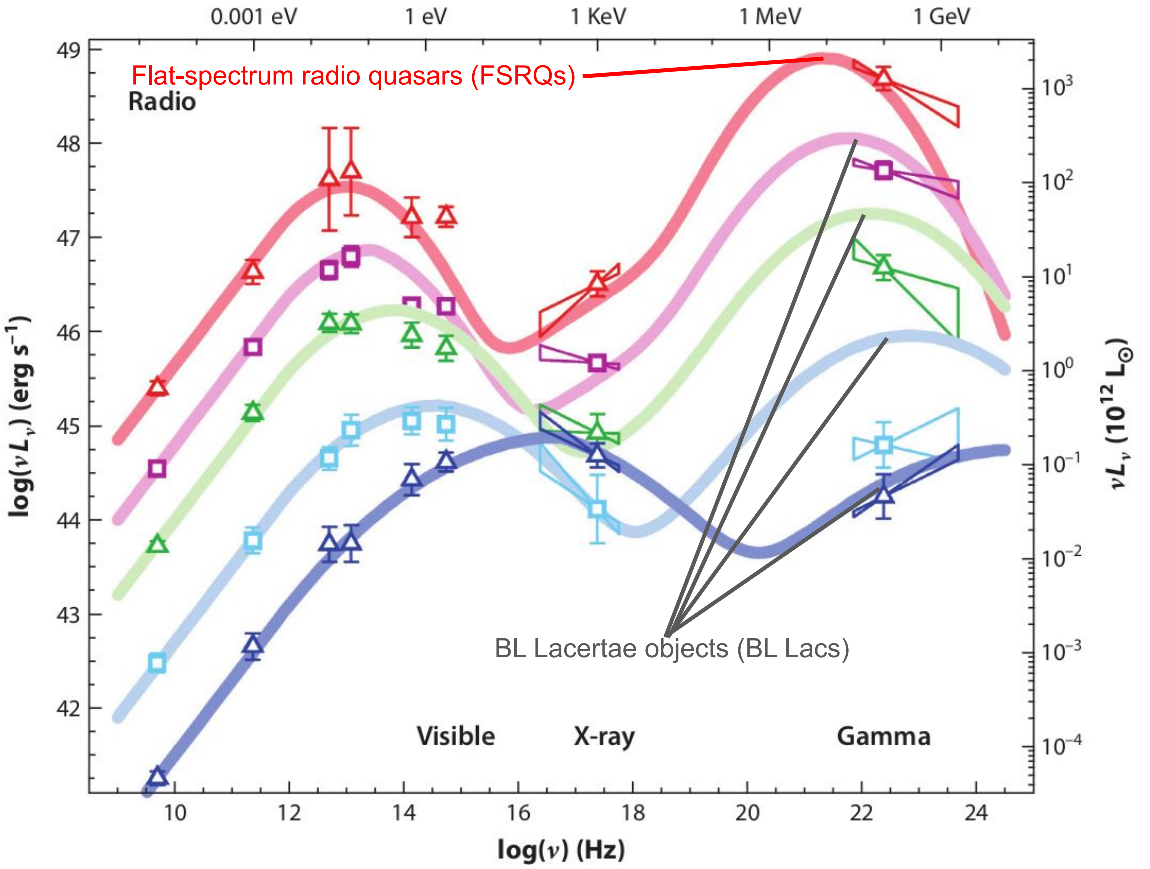

Spectral-energy distributions averaged over different sets of blazars

- the first peak occurs in different frequency ranges for different samples/luminosity classes, with most luminous sources peaking at lower frequencies;
- the peak frequency of the gamma-ray component correlates with the peak frequency of the lower energy one;
- the luminosity ratio between the high and low frequency components increases with bolometric luminosity.

Fossati et al. (1998)

Figure from Blandford et al. (2019)

Blazars

Flat-spectrum radio quasars (FSRQs)	BL Lacertae type objects (BL Lacs)
● most luminous ($L / L_{Edd} > 0.005$) ● prominent broad-line emission from broad-line regions (BLRs) ● radiatively efficient accretion in the form of geometrically thin Shakura-Sunyaev accretion disks ● stronger magnetic field in jets and more curved spectra [Anjum et al. (2020)] (?) ● jets with high bulk Lorentz factor and low magnetization [Petropoulou et al. (2023)] (?)	● luminosity $L / L_{Edd} < 0.005$ ● the peak frequencies are shifted towards higher values, no apparent emission from broad-line regions (BLRs) ● radiatively inefficient accretion in the geometrically thick advection-dominated accretion flow (ADAF, RIAF) ● weaker magnetic field in jets and less curved spectra [Anjum et al. (2020)] (?) ● jets with low bulk Lorentz factor and high magnetization [Petropoulou et al. (2023)] (?)

Fossati et al. (1998), Padovani et al. (2019), Anjum et al. (2020), Petropoulou et al. (2023)

The origin of the electromagnetic radiation in blazars

injection of charged particles (leptons / hadrons) → acceleration → cooling (production of the electromagnetic radiation)

usually substituted with a steady-state or injected particle spectrum (of already accelerated particles)

"target":

- magnetic field
- photon field
- ambient matter

- synchrotron radiation
- inverse Compton (IC) scattering (for leptons)
- Bethe-Heitler pair production (for hadrons)
- photomeson production (for hadrons)
- hadronuclear interactions with ambient matter

For a review see, e.g., Böttcher (2007) or Cerruti (2020)

The origin of the electromagnetic radiation in blazars

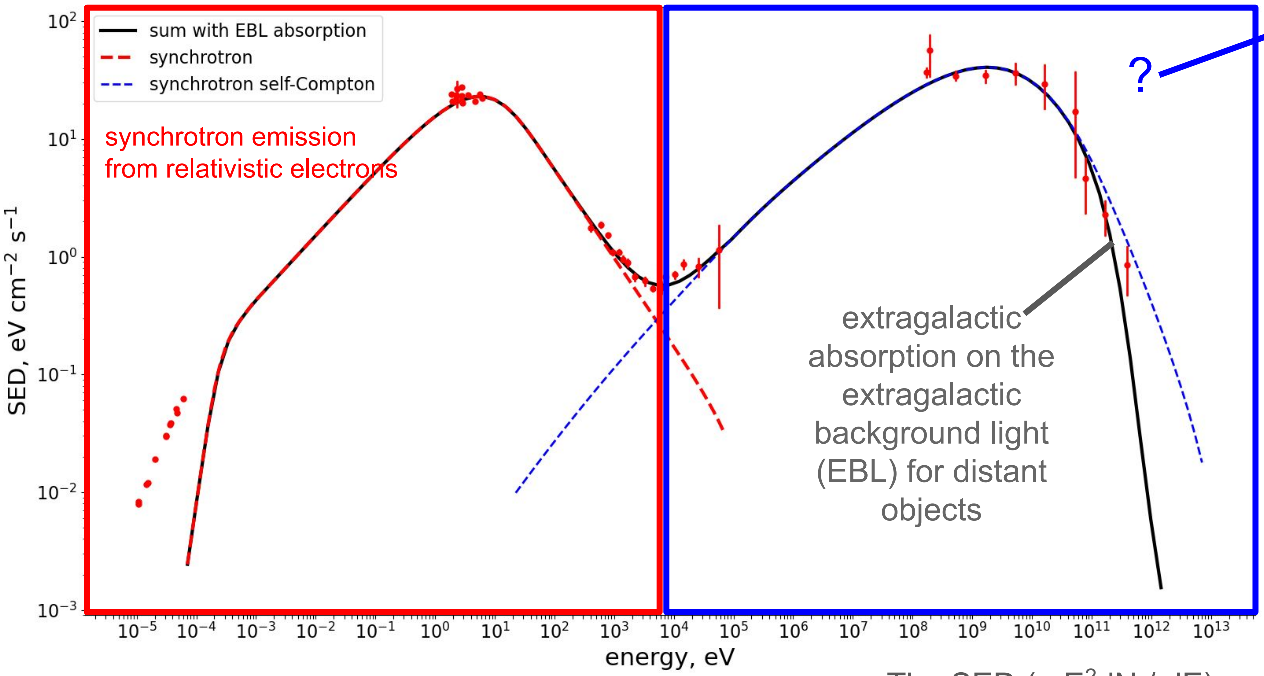

The SED (= E^2dN / dE)
of TXS 0506+056 as an example,
Data from IceCube Collaboration et al. (2018)

Different models varying with:

1) source of the electromagnetic emission (leptons / hadrons) and the mechanism of the emission (inverse Compton (IC) / synchrotron / photomeson production / Bethe-Heitler process);
2) in case of the IC scattering / photomeson production / Bethe-Heitler process: the target photon field (accretion disk radiation / broad-line region (BLR) photon field / NLR photon field / torus emission / synchrotron emission / starlight / cosmic microwave background (CMB)).

Electromagnetic cascades in photon fields

γγ-absorption

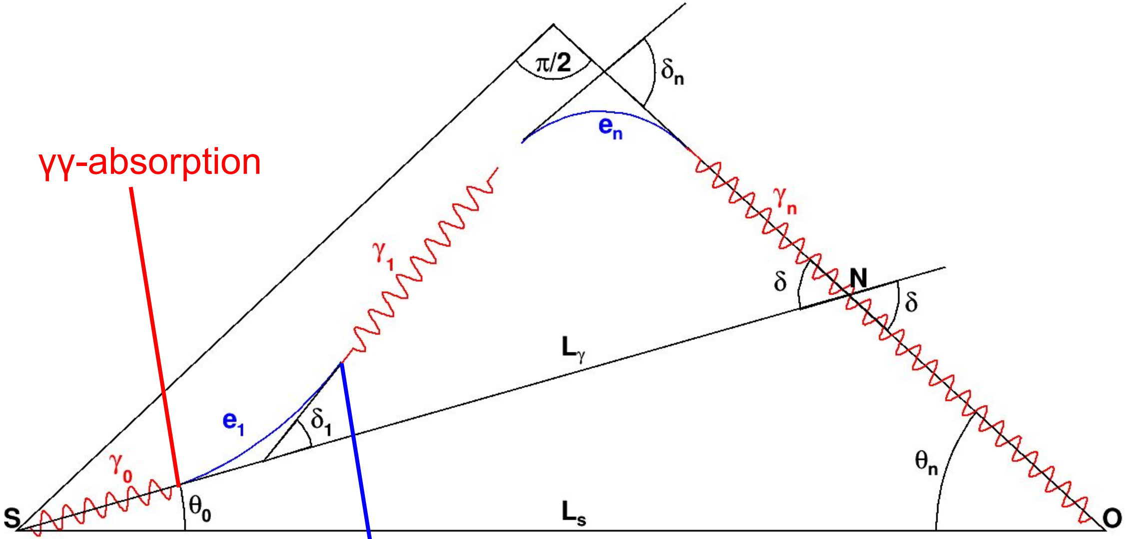

inverse Compton (IC) scattering or, in general case, synchrotron photon emission

Electromagnetic cascades can occur both in intrinsic photon fields (inside sources of gamma rays) and in the intergalactic medium. If the magnetic field is strong enough, electrons will deflect on large angles and their IC emission can be neglected (absorption-only model). In our work we assume the extragalactic absorption-only model according to the EBL model of Gilmore et al. (2012) implying $B \gtrsim 10^{-14}$ G (for correlation length of 1 Mpc).

Geometry of FSRQs

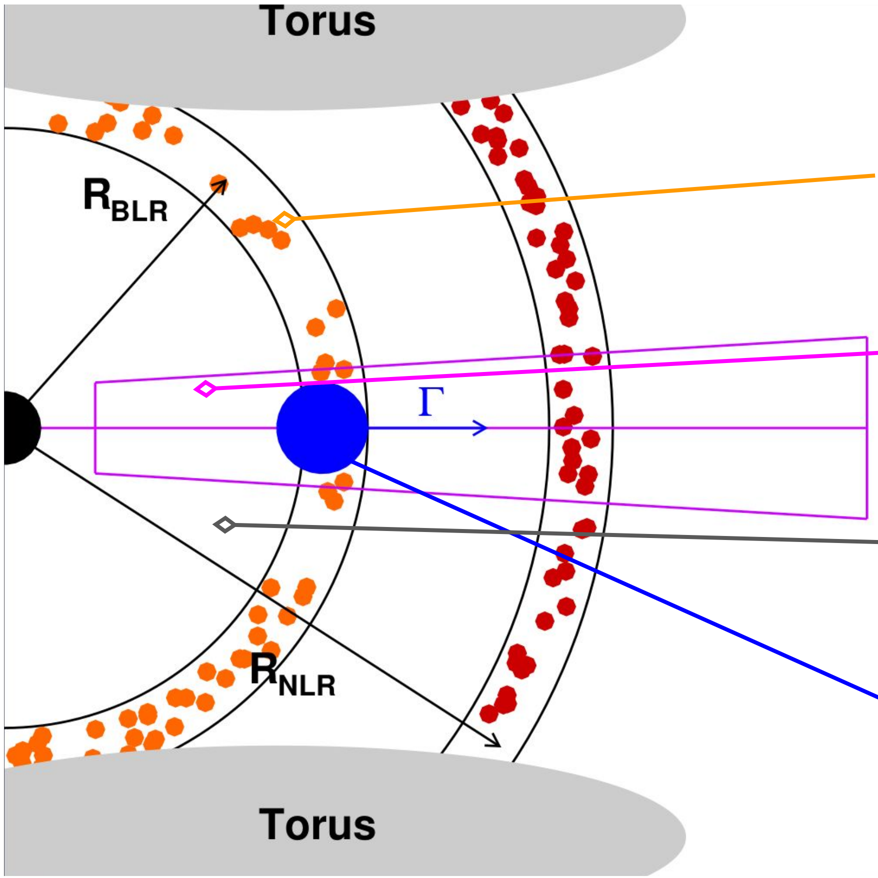

clouds of matter (or winds) in the broad line region which scatter radiation from the accretion disk near the black hole

gamma rays from FSRQs in their low states may be formed in the jet itself or from many blobs

gamma-ray emission during flares (in high states) is produced in blobs

space between the central engine and the shell of the BLR is filled with photons from the accretion disk, BLR, NLR and torus

We investigate the location of gamma-ray production site in low states of FSRQs

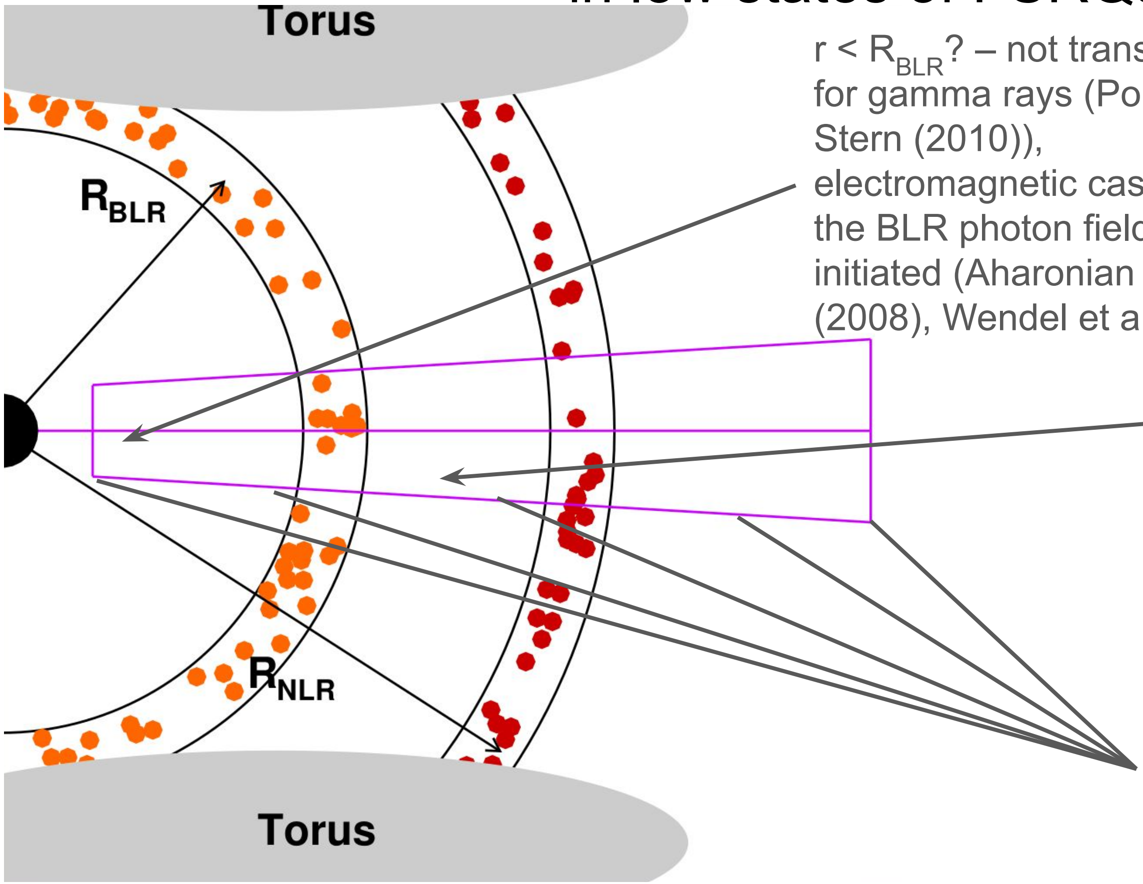

$r < R_{BLR}$? – not transparent for gamma rays (Poutanen & Stern (2010)), electromagnetic cascades on the BLR photon field may be initiated (Aharonian et al. (2008), Wendel et al. (2021))

$r \approx R_{BLR}$ or $r > R_{BLR}$? – almost transparent for gamma rays (Costamante et al. (2018))

or gamma-ray emission may be formed along the jet over large distances (Potter & Cotter (2013))

Gamma-ray emission of PKS 1510–089 in low states

A&A 619, A159 (2018)
https://doi.org/10.1051/0004-6361/201833618

Astronomy & Astrophysics

Detection of persistent VHE gamma-ray emission from PKS 1510–089 by the MAGIC telescopes during low states between 2012 and 2017

MAGIC Collaboration: V. A. Acciari[1], S. Ansoldi[2,3,24], L. A. Antonelli[4], A. Arbet Engels[5], C. Arcaro[6,7], D. Baack[8], A. Babić[9], B. Banerjee[10], P. Bangale[11], U. Barres de Almeida[11,12], J. A. Barrio[13], W. Bednarek[14], E. Bernardini[6,7,15,26], A. Berti[2,3,27], J. Besenrieder[11], W. Bhattacharyya[15], C. Bigongiari[4], A. Biland[5], O. Blanch[16], G. Bonnoli[17,18], R. Carosi[19,18], G. Ceribella[11], S. Cikota[9], S. M. Colak[16], P. Colin[11], E. Colombo[1], J. L. Contreras[13], J. Cortina[16], S. Covino[4], V. D'Elia[4], P. Da Vela[19,18], F. Dazzi[4], A. De Angelis[6,7], B. De Lotto[2,3], M. Delfino[16,28], J. Delgado[16,28], F. Di Pierro[4], E. Do Souto Espiñera[16], A. Domínguez[13], D. Dominis Prester[9], D. Dorner[20], M. Doro[6,7], S. Einecke[8], D. Elsaesser[8], V. Fallah Ramazani[21], A. Fattorini[8], A. Fernández-Barral[5,16], G. Ferrara[4], D. Fidalgo[13], L. Foffano[6,7], M. V. Fonseca[13], L. Font[22], C. Fruck[11], D. Galindo[23], S. Gallozzi[4], R. J. García López[1], M. Garczarczyk[15], M. Gaug[22], P. Giammaria[4], N. Godinović[9], D. Guberman[16], D. Hadasch[24], A. Hahn[11], T. Hassan[16], J. Herrera[1], J. Hoang[13], D. Hrupec[9], S. Inoue[24], K. Ishio[11], Y. Iwamura[24], H. Kubo[24], J. Kushida[24], D. Kuveždić[9], A. Lamastra[4], D. Lelas[9], F. Leone[4], E. Lindfors[21], S. Lombardi[4], F. Longo[2,3,27], M. López[13], A. López-Oramas[1], C. Maggio[22], P. Majumdar[10], M. Makariev[25], G. Maneva[25], M. Manganaro[9], K. Mannheim[20], L. Maraschi[4], M. Mariotti[6,7], M. Martínez[16], S. Masuda[24], D. Mazin[11,24], M. Minev[25], J. M. Miranda[17,18], R. Mirzoyan[11], E. Molina[23], A. Moralejo[16], V. Moreno[22], E. Moretti[16], P. Munar-Adrover[22], V. Neustroev[21], A. Niedzwiecki[14], M. Nievas Rosillo[13], C. Nigro[15,⋆], K. Nilsson[21], D. Ninci[16], K. Nishijima[24], K. Noda[24], L. Nogués[16], S. Paiano[6,7], J. Palacio[16], D. Paneque [11], R. Paoletti[17,18], J. M. Paredes[23], G. Pedaletti[15], P. Peñil[13], M. Peresano[2,3], M. Persic[2,3,29], P. G. Prada Moroni[19,18], E. Prandini[6,7], I. Puljak[9], J. R. Garcia[11], W. Rhode[8], M. Ribó[23], J. Rico[16], C. Righi[4], A. Rugliancich[19,18], L. Saha[13], T. Saito[24], K. Satalecka[15], T. Schweizer[11], J. Sitarek[14,⋆], I. Šnidarić[9], D. Sobczynska[14], A. Somero[1], A. Stamerra[4], M. Strzys[11], T. Surić[9], F. Tavecchio[4], P. Temnikov[25], T. Terzić[9], M. Teshima[11,24], N. Torres-Albà[23], S. Tsujimoto[24], J. van Scherpenberg[11], G. Vanzo[1], M. Vazquez Acosta[1], I. Vovk[11], J. E. Ward[16], M. Will[11], D. Zarić[9];
Fermi-LAT Collaboration: J. Becerra González[1,⋆];
and C. M. Raiteri[30], A. Sandrinelli[31,32], T. Hovatta[34], S. Kiehlmann[33], W. Max-Moerbeck [35], M. Tornikoski[36], A. Lähteenmäki [36,37,38], J. Tammi[36], V. Ramakrishnan[36], C. Thum[39], I. Agudo[40], S. N. Molina [40], J. L. Gómez[40], A. Fuentes[40], C. Casadio[41], E. Traianou[41], I. Myserlis[41], and J.-Y. Kim[41]

(Affiliations can be found after the references)

Received 12 June 2018 / Accepted 31 August 2018

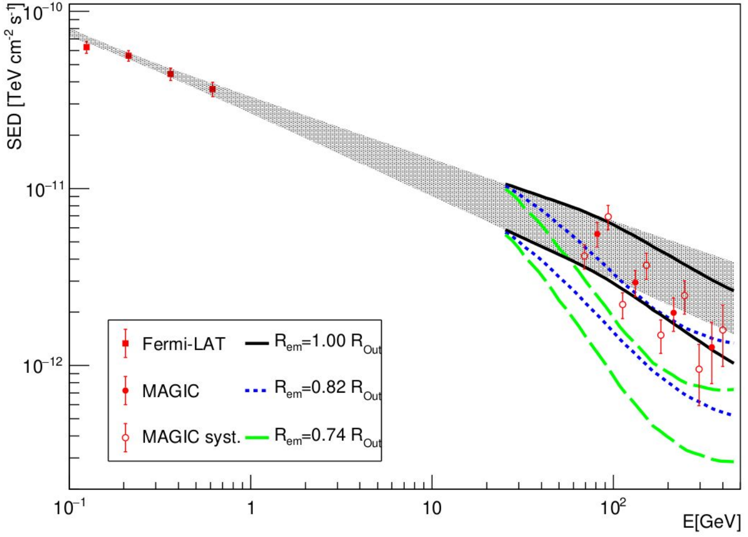

Fig. 7. Gamma-ray spectrum of PKS 1510–089 during low state measured by *Fermi*-LAT (squares) and MAGIC (filled circles). The 68% confidence band of the extrapolation of the *Fermi*-LAT spectrum to sub-TeV energies is shown as a gray shaded region. The extrapolation in the MAGIC energy range assuming absorption in BLR following Böttcher & Els (2016) for the emission region located at the distance of 1, 0.82, and 0.74 of the outer radius of the broad line region is shown with black solid, blue dotted, and green dashed lines, respectively. Empty circles show the effect of the systematic uncertainties on the MAGIC spectrum.

Acciari et al. (2018) constraints on the location of the gamma-ray emitting zone are based on the *interpolation* of *Fermi*-LAT data from the same nights the MAGIC observatory carried out SED measurements of PKS 1510-089 blazar.

In our work, we obtain the *Fermi*-LAT SED averaged over the whole period of the PKS 1510-089 low state.

2 day-binned *Fermi*-LAT light curve of PKS 1510-089, 100 MeV < E < 300 GeV

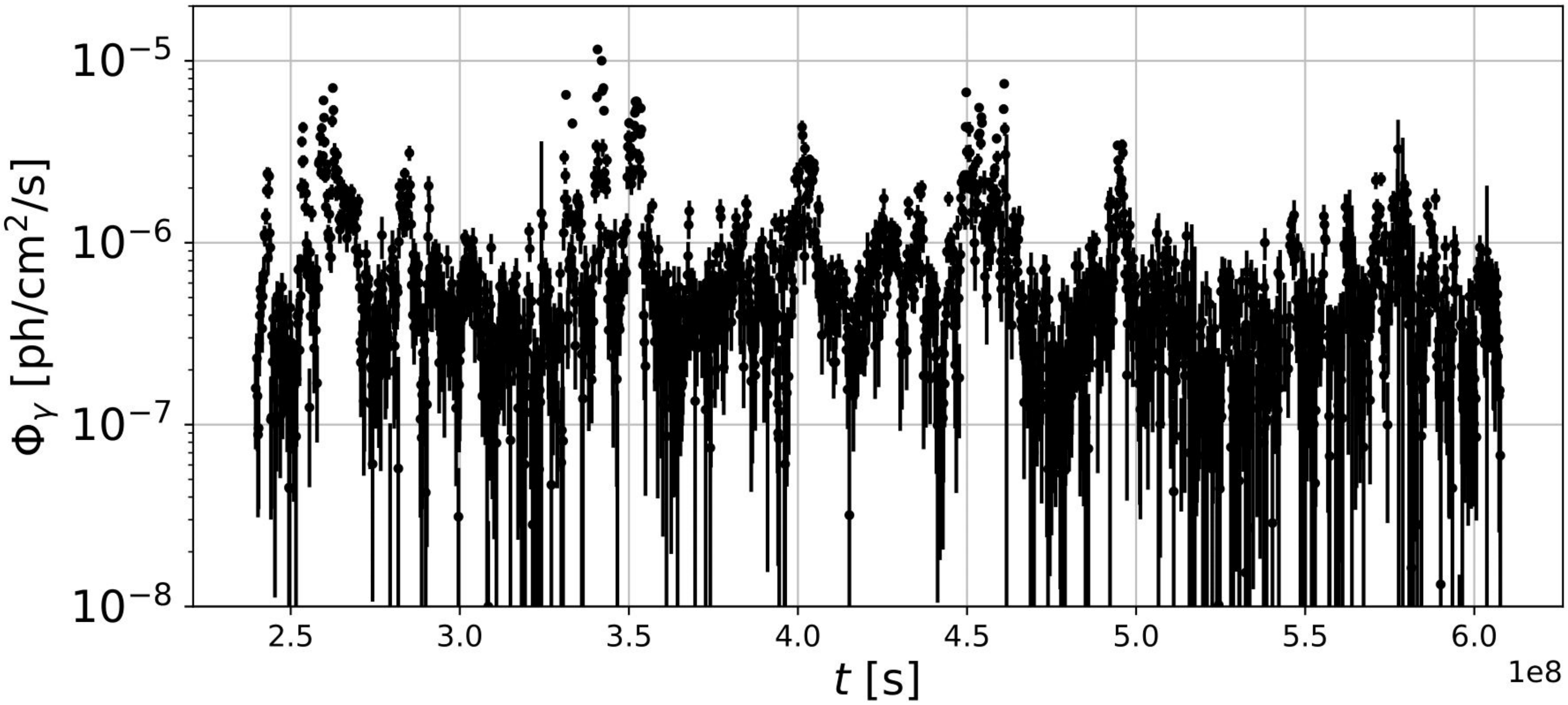

Our PKS 1510–089 low state selection

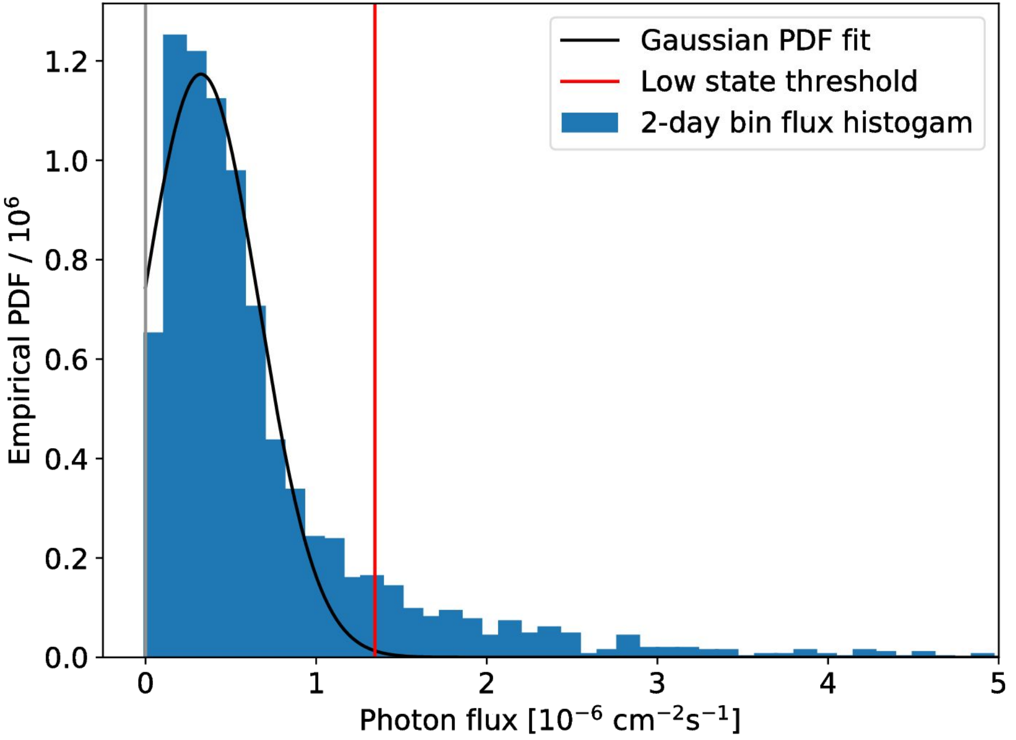

The empirical probability density function of the observed photon flux in each 2-day bin fitted with the Gaussian pdf (right wing), the photon flux at 3-sigma deviation is chosen as the low state threshold.

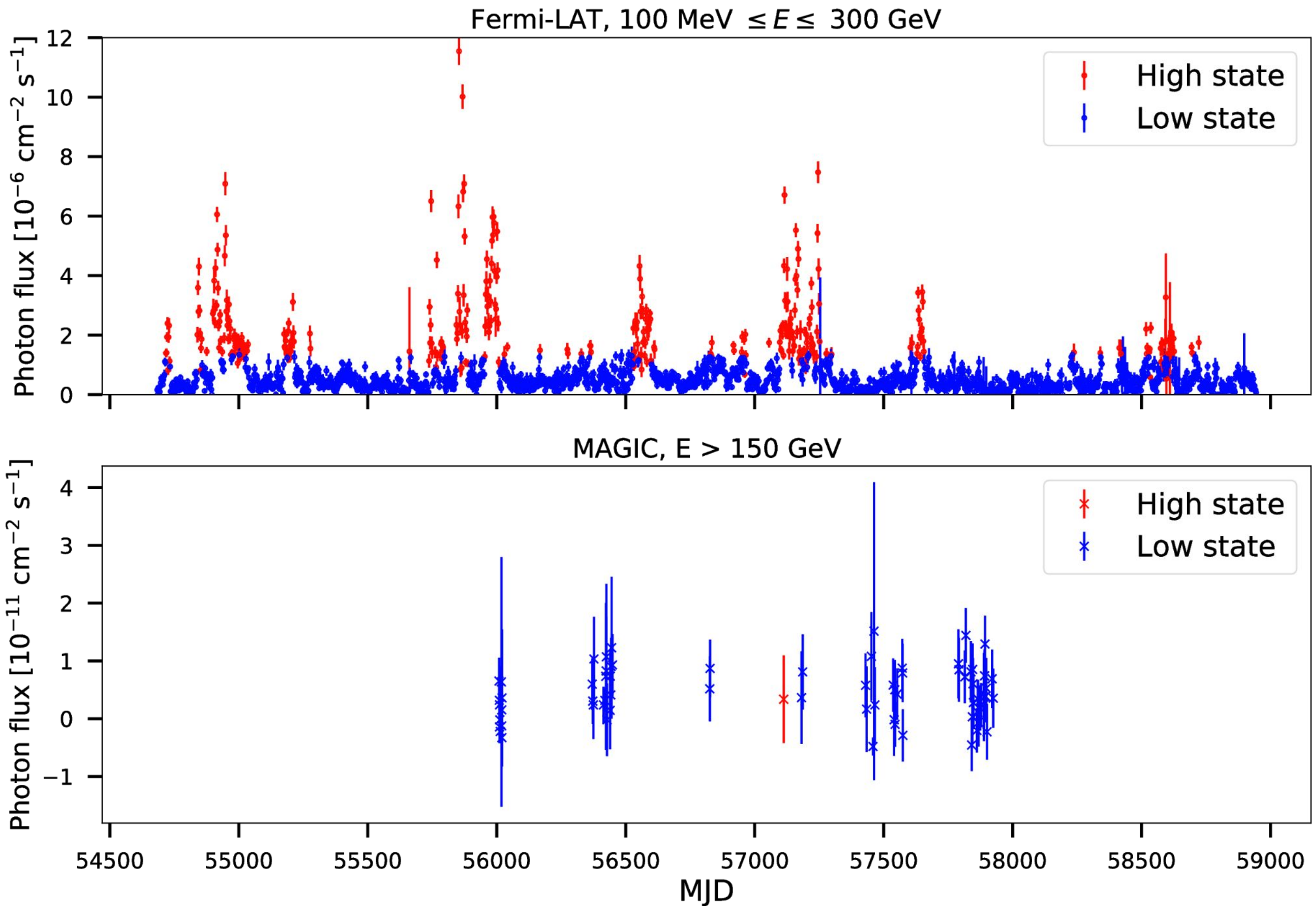

Fermi-LAT light curve – our work

MAGIC light curve – from Acciari et al. (2018)

Spectral-energy distribution (SED = $E^2 dN/dE$) averaged over PKS 1510–089 low state periods

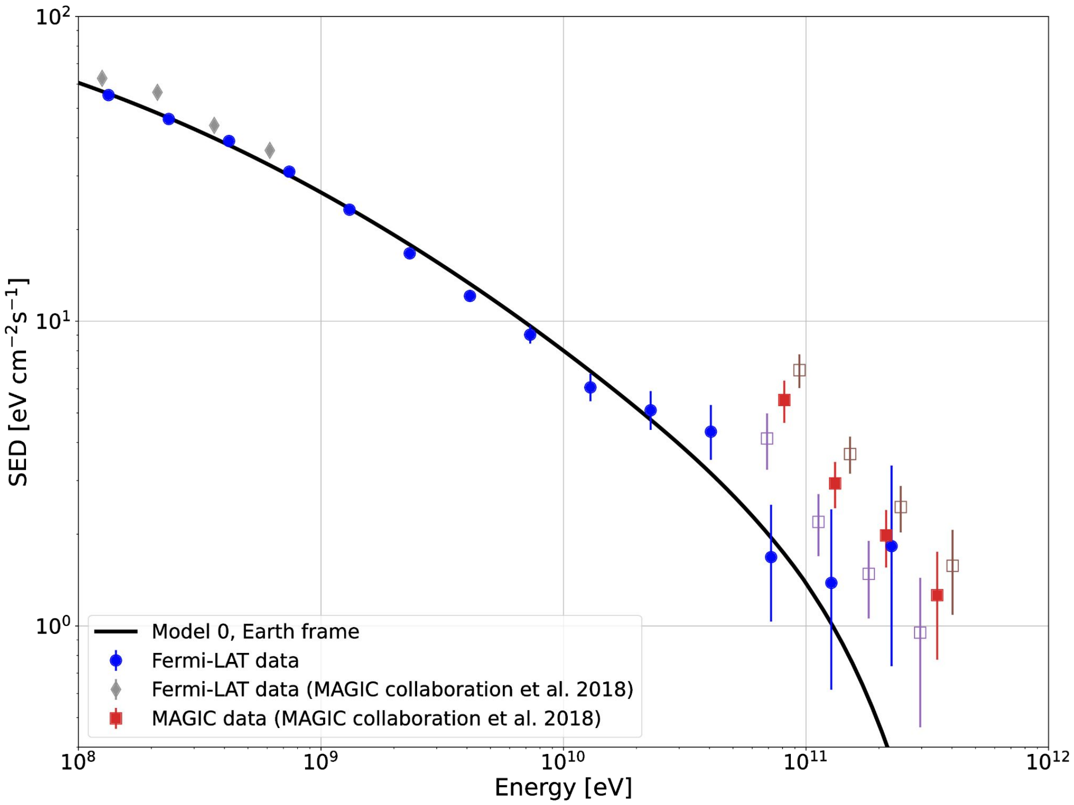

Baseline model (model 0)

$$\frac{dN}{dE}(E) = \underbrace{C\,(E\,(1+z)/E_{ref})^{-(\alpha + \beta \ln(E\,(1+z)/E_{ref}))}}_{\text{injection}}\ \underbrace{\exp[-\tau_{EBL}(E)]\,/\,(1+z)}_{\text{extragalactic propagation}}$$

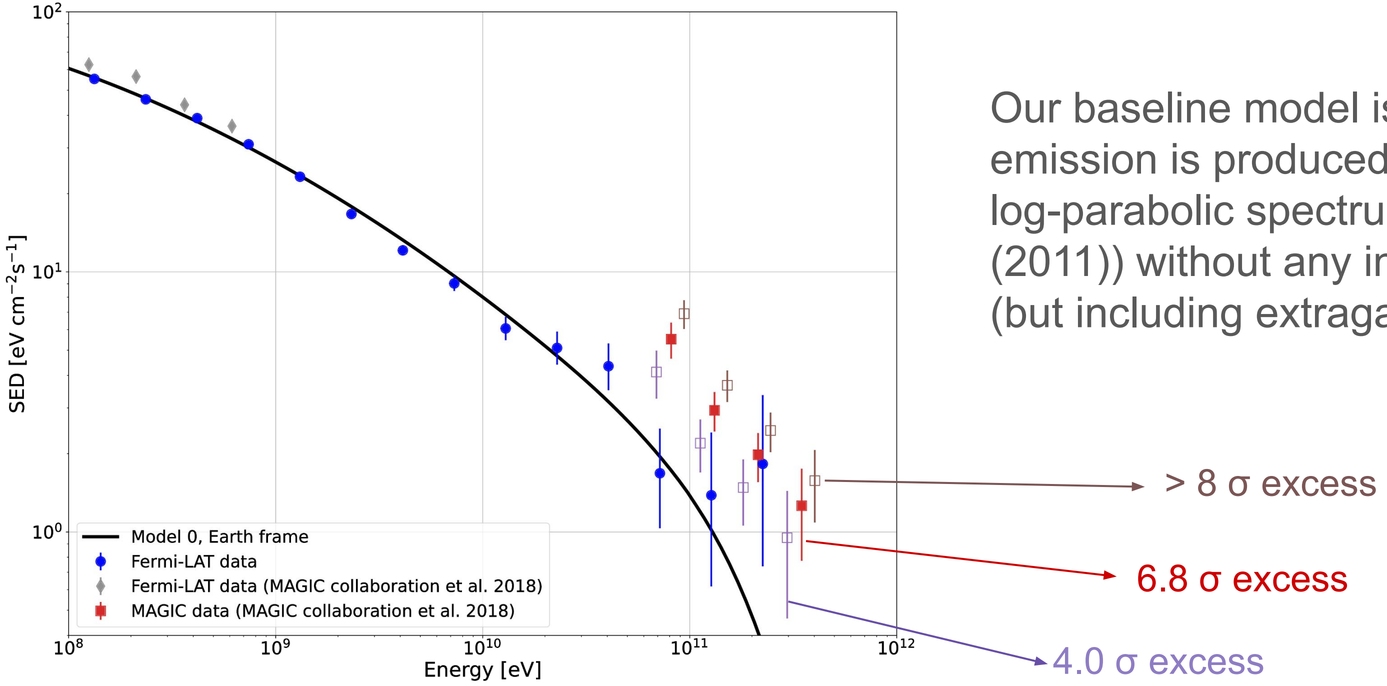

Our baseline model is that gamma-ray emission is produced with the log-parabolic spectrum (Tramacere et al. (2011)) without any intrinsic absorption (but including extragalactic absorption).

Geometry of the FSRQ PKS 1510–089 adopted in our model

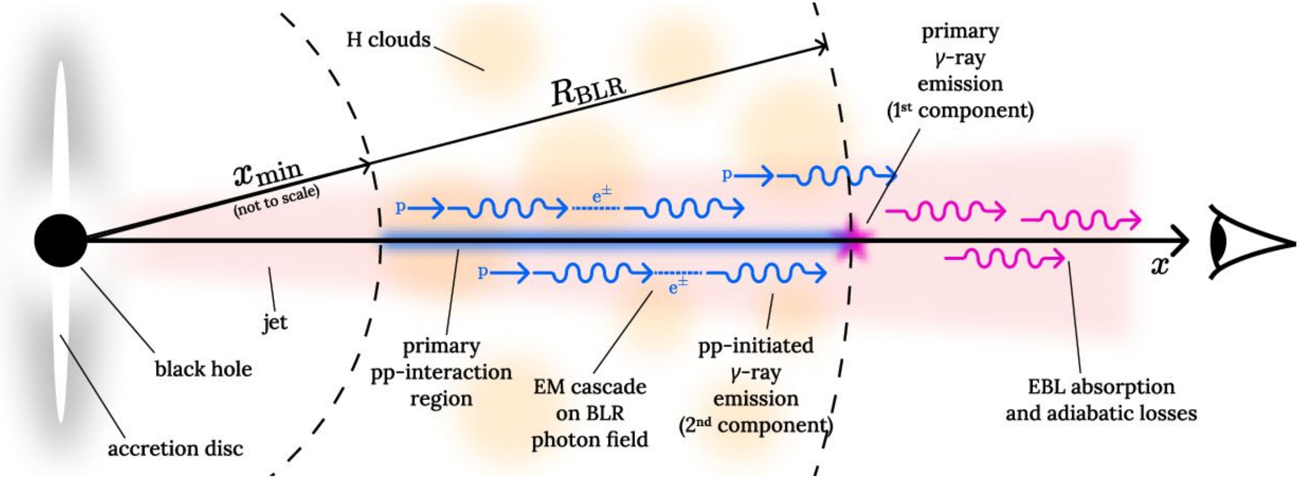

We propose the model according to the scenario of Dar & Laor (1997), but in our scenario protons with energies from 10 TeV to 1000 TeV are constantly interacting with some matter in the BLR producing very high-energy gamma rays which initiate the electromagnetic cascade on the BLR photon field at $0.9R_{BLR}$ from the central engine.

1) ~ 100 GeV gamma ray observations ⇒ $\tau_{\gamma\gamma}$(~100 GeV) < 2−3

2) ⇒ background photon field energies are $E_b \lesssim 10$ eV

3) ⇒ for the photomeson production, the threshold is high: ~5 PeV × $(E_b /10\ \mathrm{eV})^{-1}$

4) But for pp interactions the threshold is only 1.22 GeV, $\tau_{pp} \sim 5\times10^{-3}\times(N_c / 10^{23}\ \mathrm{cm}^{-2})$

5) Possibility to obtain neutrinos with energies in the range of 1 TeV…100 TeV for proton energies from 10 TeV to 1 PeV.

BLR photon field according to Cloudy simulation
www.nublado.org

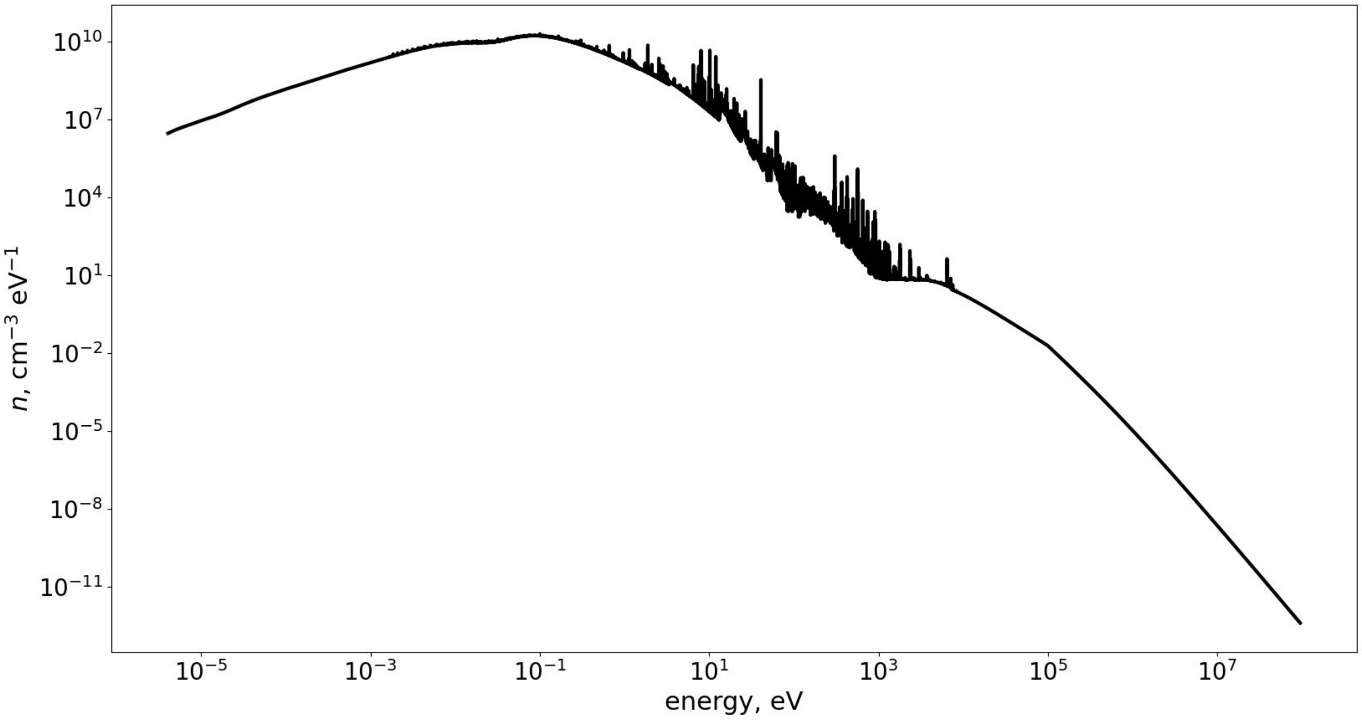

Assumed AGN luminosity L_{AGN} = 10^{46} erg / s, BLR radius R_{BLR} = 0.036 pc = 10^{17} cm (from spectroscopic reverberation mapping, Rakshit (2020)), matter column density N_c = 10^{23} cm^{-2}, cloud covering factor f = 0.1, other parameters are set to default

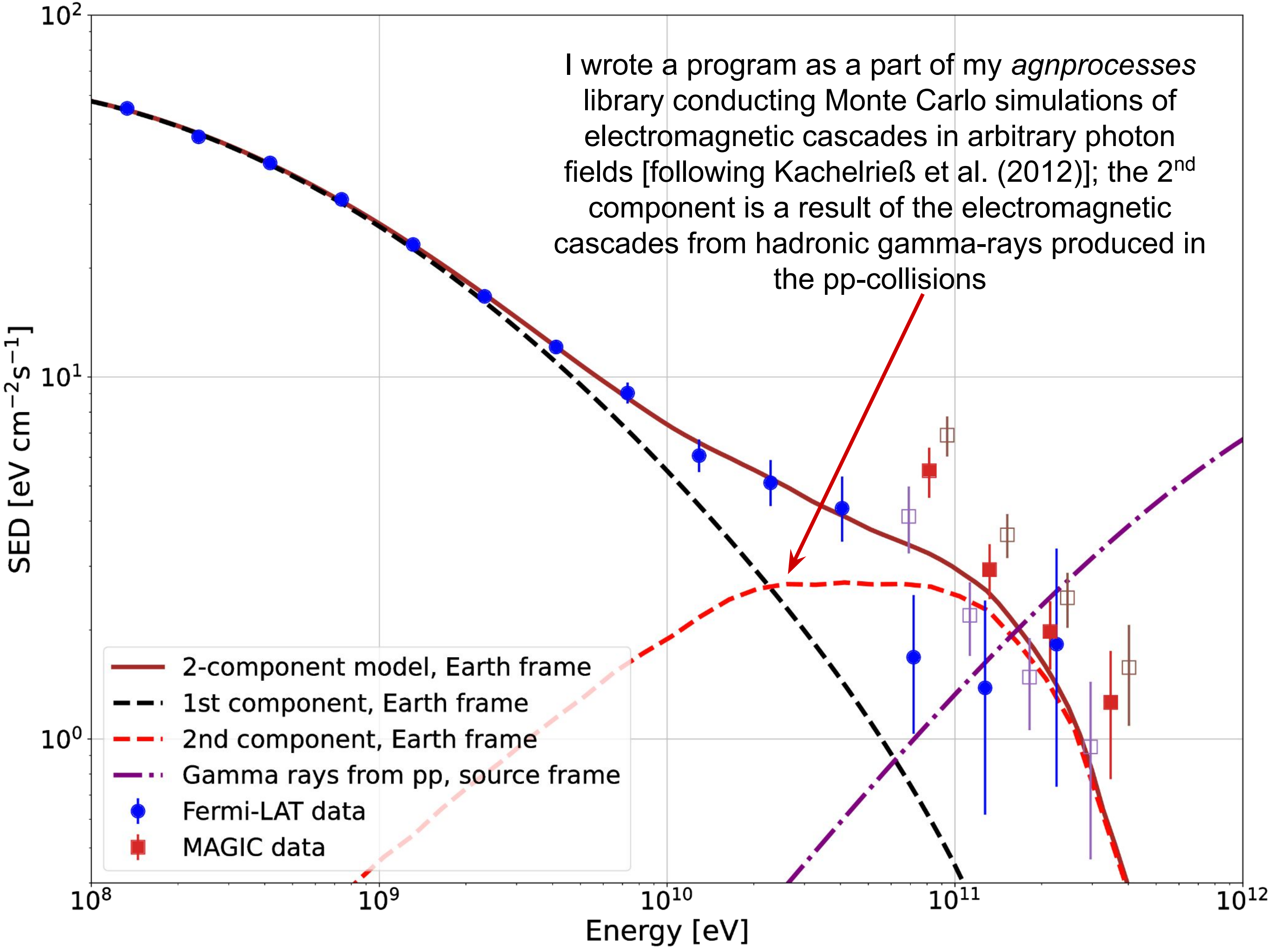
I wrote a program as a part of my *agnprocesses* library conducting Monte Carlo simulations of electromagnetic cascades in arbitrary photon fields [following Kachelrieß et al. (2012)]; the 2nd component is a result of the electromagnetic cascades from hadronic gamma-rays produced in the pp-collisions
2-component model, Earth frame
1st component, Earth frame
2nd component, Earth frame
Gamma rays from pp, source frame
Fermi-LAT data
MAGIC data
SED [eV cm^{-2}s^{-1}]
Energy [eV]
10^{2}
10^{1}
10^{0}
10^{8}
10^{9}
10^{10}
10^{11}
10^{12}

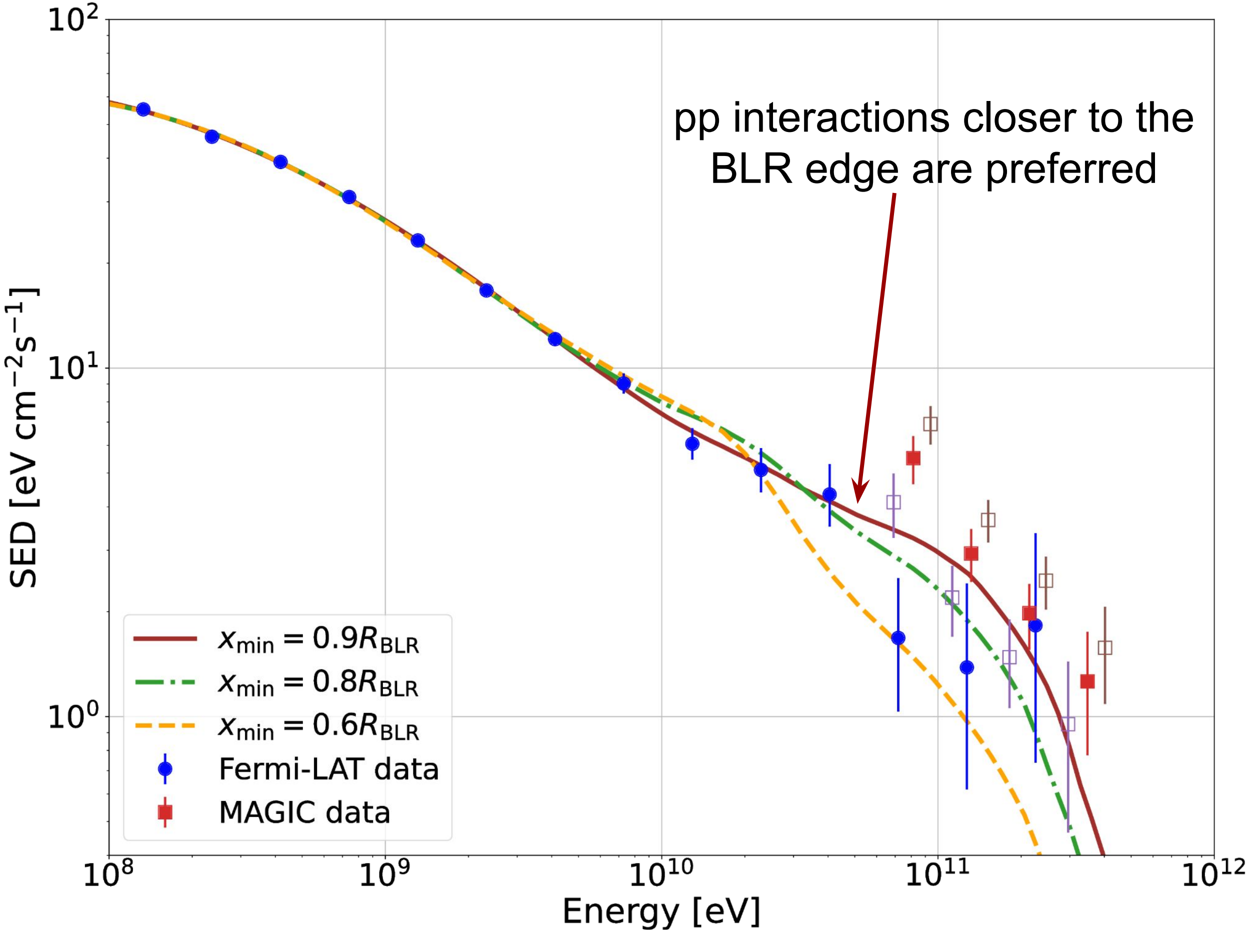

Estimated IceCube neutrino signal for 6 years is ~15 neutrinos given the atmospheric background of ~30 events. In case of rapid increase of the BLR matter column density N_c, neutrino flares can be produced without a counterpart *Fermi*-LAT gamma-ray flare ⇒ this is a possible explanation of the TXS 0506+056 neutrino flare in 2014-2015.

Conclusions

1. In the energy range from 100 MeV to 20 GeV, the observed SED of PKS 1510–089 averaged over low states is well described with a log-parabolic gamma-ray spectrum.
2. At E > 20 GeV some excess of gamma rays is apparent.
3. A possible scenario that could explain this excess includes primary proton interactions with BLR matter resulting in the production of secondary gamma rays.
4. If this scenario is confirmed, it would provide evidence for: 1) acceleration of protons or nuclei in blazar jets, 2) interaction of these hadrons with the BLR matter in FSRQs, 3) the production of sub-TeV gamma rays, and 4) the production of 1 TeV – 100 TeV neutrinos in FSRQs near the edge of the BLR.

Thank you for your attention!

References

- Acciari et al., A&A, 619, A159 (2018)
- Aharonian et al., MNRAS, 387, 3, 1206-1214 (2008)
- Anjum et al., ApJ, 898, 48 (2020)
- Blandford et al., Annu. Rev. Astron. Astrophys., 57, 467–509 (2019)
- Böttcher, Astrophysics and Space Science, 309, 1-4, 95-104 (2007)
- Cerruti, Galaxies, 8, 4, 72 (2020)
- Costamante et al., MNRAS, 477, 4749–4767 (2018)
- Dar & Laor, ApJ, 478, 1, L5-L8 (1997)
- Fossati et al., MNRAS, 299, 2, 433-448 (1998)
- Gilmore et al., MNRAS, 422, 3189-3207 (2012)
- Kachelrieß et al., Computer Physics Communications, 183, 1036-1043 (2012)
- Padovani et al., MNRAS, 484, 1, L104-L108 (2019)
- Petropoulou et al., MNRAS, 518, 2719-2734 (2023)
- Potter & Cotter, MNRAS, 431, 2, 1840-1852 (2013)
- Poutanen & Stern, ApJ Lett., 717, 2, L118-L121 (2010)
- Rakshit, A&A, 642, A159 (2020)
- The IceCube Collaboration et al., Science, 361, eaat1378 (2018)
- Wendel et al., ApJ, 917, 1, 32 (2021)

Backup slides

$$L_{\gamma-2-\mathrm{iso}} = 3.5 \times 10^{46}\ \mathrm{erg\ s^{-1}}$$

$$\tau_{pp} = 5 \times 10^{-3},\ f_\gamma = 0.2$$

$$L_{p-\mathrm{iso}} = L_{\gamma-2-\mathrm{iso}} / (\tau_{pp}\, f_\gamma) = 3.5 \times 10^{49}\ \mathrm{erg\ s^{-1}}$$

$$\begin{aligned} L_{\mathrm{p}} &\approx L_{\mathrm{p-iso}} \left[1 - \cos(\theta_{\mathrm{jet}})\right] \left(\frac{N_{\mathrm{c}}}{10^{23}\ \mathrm{cm}^{-2}} \right)^{-1} \\ &\approx L_{\mathrm{p-iso}} \frac{\theta_{\mathrm{jet}}^2}{2} \left(\frac{N_{\mathrm{c}}}{10^{23}\ \mathrm{cm}^{-2}} \right)^{-1}, \end{aligned}$$

$$L_p \approx 5 \times 10^{45}\ \mathrm{erg\ s^{-1}},\ \text{for } \theta_{jet} = 1^\circ,\ N_c = 10^{23}\ \mathrm{cm^{-2}}$$

Scatter plot of PKS 1510-089 spectral parameters

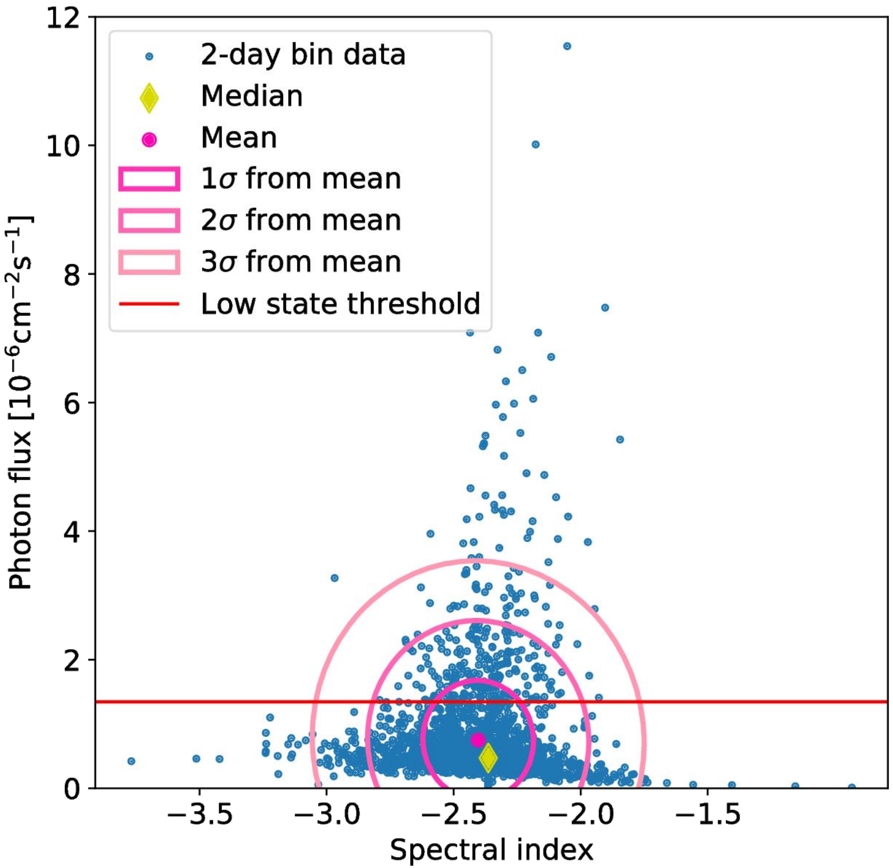

γγ optical depth in the whole BLR region